

Synthesis and Characterization of Volatile Monomeric Copper(II) Fluoroalkoxides

Patrick M. Jeffries, Scott R. Wilson, and Gregory S. Girolami*

School of Chemical Sciences and Materials Research Laboratory, University of Illinois at Urbana-Champaign, 505 South Mathews Avenue, Urbana, Illinois 61801

Received February 2, 1992

The reaction of $[\text{Cu}(\text{OMe})_2]_n$ with a fluorinated alcohol in the presence of an amine has afforded a series of new copper(II) fluoroalkoxides: $\text{Cu}(\text{hfip})_2(\text{tmed})$ (**2**), $\text{Cu}(\text{hfip})_2(\text{teed})$ (**3**), $\text{Cu}(\text{hfip})_2(\text{bipy})$ (**4**), $\text{Cu}(\text{hfip})_2(\text{py})_2$ (**5**), $\text{Cu}(\text{hftb})_2(\text{tmed})$ (**6**), $\text{Cu}(\text{hftb})_2(\text{bipy})$ (**7**), and $\text{Cu}(\text{hftb})_2(\text{py})_2$ (**8**), where hfip = hexafluoroisopropoxy, hftb = hexafluoro-*tert*-butoxy, tmed = *N,N,N',N'*-tetramethylethylenediamine, teed = *N,N,N',N'*-tetraethylethylenediamine, bipy = bipyridine, and py = pyridine. Compounds **5** and **8** have also been prepared by the reaction of CuBr_2 with $\text{Na}(\text{hfip})$ or $\text{Na}(\text{hftb})$ and pyridine. Crystallographic analyses of **2** and **6** reveal that both compounds are monomeric and assume tetrahedrally-distorted square-planar geometries. The dihedral angles between the CuN_2 and CuO_2 planes are 16.1° for **2** and 40.6° for **6**. The average Cu–O distances are 1.903 (3) Å in **2** and 1.884 (3) Å in **6**, and the average Cu–N distances are 2.035 (5) Å in **2** and 2.064 (3) Å in **6**. EPR and UV–vis studies indicate that the degree of distortion increases in the order $4 < 2 < 3 < 7 < 5 < 6 < 8$. The increase in the degree of distortion is attributed to the greater steric crowding in the latter molecules. Interestingly, these compounds are relatively resistant to hydrolysis: aqueous solutions of **2** are stable in air at room temperature and hydrolyze to copper(II) oxide only when the solutions are refluxed. Compounds **2**, **3**, **4**, **6**, and **7** are volatile, and thus are potential metal–organic chemical vapor deposition (MOCVD) precursors. Sublimation of **2** and passage of the resulting vapor over substrates heated to 300°C result in the deposition of copper metal. These deposits are noncrystalline and consist of granules having diameters of 0.1–0.4 μm . Crystal data: for $\text{Cu}(\text{hfip})_2(\text{tmed})$ (**2**), space group $P2_1/c$, monoclinic, $a = 9.454$ (1) Å, $b = 15.045$ (2) Å, $c = 14.197$ (6) Å, $\beta = 105.65$ (2) $^\circ$, $V = 1944$ (1) Å³, $Z = 4$, $R_F = 0.040$ and $R_{wF} = 0.052$ for 334 variables and 2060 data; for $\text{Cu}(\text{hftb})_2(\text{tmed})$ (**6**), space group $I2/a$, monoclinic, $a = 13.601$ (3) Å, $b = 9.567$ (2) Å, $c = 16.562$ (5) Å, $\beta = 106.56$ (2) $^\circ$, $V = 2066$ (2) Å³, $Z = 4$, $R_F = 0.043$ and $R_{wF} = 0.037$ for 190 variables and 1427 data.

Introduction

The fabrication of thin films of high-temperature superconductors by metal–organic chemical vapor deposition (MOCVD) is an area of rapidly growing interest.^{1–4} Because no volatile single precursor exists which contains all of the requisite elements, these deposition processes involve simultaneous passage of several precursors through the deposition zone. Copper is the key constituent in the high-temperature superconductors, and as a result, the deposition of copper and copper oxide films is under active investigation.

Metal alkoxides are popular MOCVD precursors to metal oxide films, because they are often reasonably volatile and undergo clean conversion to the product phase under MOCVD conditions.^{5–7} However, the homoleptic copper(II) alkoxides $[\text{Cu}(\text{OR})_2]_n$ ($R = \text{Me}, \text{Et}, i\text{-Pr}, s\text{-Bu}, t\text{-Bu}, t\text{-Am}$) are not suitable as MOCVD precursors because they are polymeric and nonvolatile.⁸ Several investigators have overcome this difficulty by employing functionalized polydentate alkoxide ligands, and copper(II) amino–alkoxide complexes such as $\text{Cu}[\text{O}(\text{CH}_2)_2\text{N}(\text{Et})_2]_2$,⁹ $\text{Cu}[\text{O}(\text{CH}_2)_2\text{NMe}_2]_2$,¹⁰ $\text{Cu}[\text{OCHMeCH}_2\text{NMe}_2]_2$,¹⁰ and

$\text{Cu}[\text{O}(\text{CH}_2)_2\text{NMe}(\text{CH}_2)_2\text{NMe}_2]_2$ ¹⁰ have been prepared that sublime at temperatures between 60 and 110°C in vacuum. The solid-state pyrolysis of $\text{Cu}[\text{O}(\text{CH}_2)_2\text{NMe}_2]_2$ and $\text{Cu}[\text{OCHMeCH}_2\text{NMe}_2]_2$ produces Cu–CuO–Cu₂O mixtures and copper metal, respectively.¹⁰ Because it has proven difficult to prepare volatile copper(II) compounds with unidentate alkoxide groups,^{11–13} most workers have employed complexes with other ligands, especially β -diketonates, as CVD precursors to copper-containing phases.^{14–16}

We have recently reported the deposition of copper metal and copper(I) oxide from a copper(I) alkoxide precursor, tetrameric copper(I) *tert*-butoxide.⁵ We now present the synthesis of several new volatile copper(II) complexes with unidentate fluoroalkoxide ligands and an investigation of their utility as MOCVD precursors to copper-containing phases.

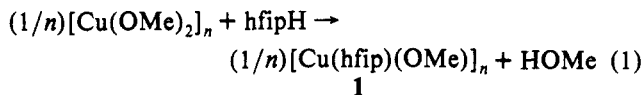
Results and Discussion

Synthesis of New Copper(II) Fluoroalkoxide Complexes.

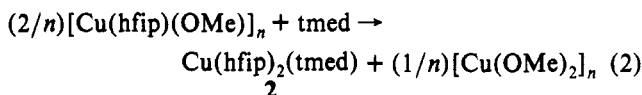
Copper(II) methoxide reacts with hexafluoroisopropyl alcohol (hfipH) in refluxing benzene to form an insoluble turquoise-colored solid of approximate stoichiometry $[\text{Cu}(\text{hfip})(\text{OMe})]_n$ (**1**); the actual molecular formula of **1** based on microanalytical data is nearer to $[\text{Cu}(\text{hfip})_{0.8}(\text{OMe})_{1.2}]_n$. This stoichiometry is obtained even after prolonged refluxing in the presence of excess hfipH, and complete ligand exchange to give the binary alkoxide $\text{Cu}(\text{hfip})_2$ has not been achieved.

- Zhang, J. M.; Wessels, B. W.; Tonge, L. M.; Marks, T. J. *Appl. Phys. Lett.* **1990**, *56*, 976–978.
- Singh, R.; Sinha, S.; Hsu, N. J.; Chou, P. J. *Appl. Phys.* **1990**, *67*, 1562–1565.
- Zhang, K.; Boyd, E. P.; Kwak, B. S.; Wright, A. C.; Erbil, A. *Appl. Phys. Lett.* **1989**, *55*, 1258–1260.
- Zhang, J. M.; Marcy, H. O.; Tonge, L. M.; Wessels, B. W.; Marks, T. J.; Kannewurf, C. R. *Appl. Phys. Lett.* **1989**, *55*, 1906–1908.
- Jeffries, P. M.; Girolami, G. S. *Chem. Mater.*, in press.
- Hough, R. L. *Proc. Int. Conf. Chem. Vap. Deposition*, **3rd** **1972**, 232–241.
- Bradley, D. C. *Chem. Rev.* **1989**, *89*, 1317–1322.
- Singh, J. V.; Baranwal, B. P.; Mehrotra, R. C. Z. *Anorg. Allg. Chem.* **1981**, *477*, 235–240.
- Horowitz, H. S.; McLain, S. J.; Sleight, A. W.; Druliner, J. D.; Gai, P. L.; VanKavelaar, M. J.; Wagner, J. L.; Biggs, B. D.; Poon, S. J. *Science* **1989**, *243*, 66–69.

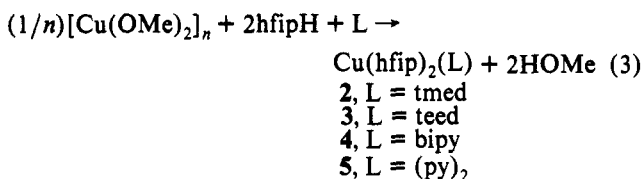
- Goel, S. C.; Kramer, K. S.; Chiang, M. Y.; Buhro, W. E. *Polyhedron* **1990**, *9*, 611–613.
- Gross, M. E. *J. Electrochem. Soc.* **1991**, *138*, 2422–2426.
- Purdy, A. P.; George, C. F. *Inorg. Chem.* **1991**, *30*, 1969–1970.
- Purdy, A. P.; George, C. F.; Callahan, J. H. *Inorg. Chem.* **1991**, *30*, 2812–2819.
- Van Hemert, R. L.; Spendlove, L. B.; Sievers, R. E. *J. Electrochem. Soc.* **1965**, *112*, 1123–1126.
- Shin, H. K.; Chi, K. M.; Hampden-Smith, M. J.; Kodas, T. T.; Farr, J. D.; Paffett, M. F. *Adv. Mater.* **1991**, *3*, 246–248.
- Norman, J. A. T.; Muratore, B. A.; Dyer, P. N.; Roberts, D. A.; Hochberg, A. K. *J. Phys. IV* **1991**, *1* (C2), 271–278.



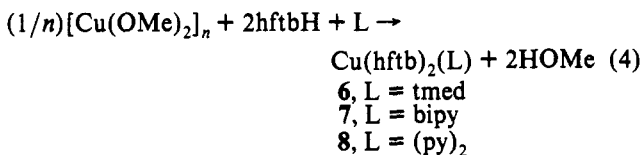
Although treatment of copper(II) methoxide with hfipH does not lead to the formation of $\text{Cu}(\text{hfip})_2$, the reaction of the mixed-ligand species **1** with *N,N,N',N'*-tetramethylethylenediamine (tmed) in diethyl ether results in redistribution of the coordinated ligands and formation of the bis(hexafluoroisopropoxo) complex $\text{Cu}(\text{hfip})_2(\text{tmed})$ (**2**). Subsequently, it was discovered that **2** can



be produced in one step by the addition of hfipH and tmed to $[\text{Cu}(\text{OMe})_2]_n$ in diethyl ether at room temperature. This one-step reaction also works for several other amines such as *N,N,N',N'*-tetraethylethylenediamine (teed), 2,2'-bipyridine (bipy), and pyridine (py) to yield the corresponding hfip complexes.

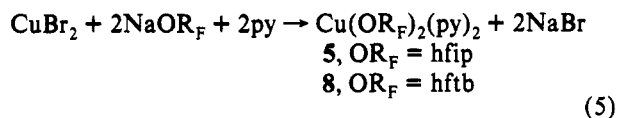


Analogous compounds with hexafluoro-*tert*-butoxide ligands can be synthesized similarly by treatment of copper(II) methoxide with hexafluoro-*tert*-butyl alcohol (hftbH) and the appropriate amine in diethyl ether.



Compound **6** can be synthesized in higher yields in refluxing benzene. The reaction of $\text{Ba}[\text{Cu}(\text{hftb})_3]_2$ with tmed has also been reported to afford compound **6**.¹² Somewhat unexpectedly, it has not been possible to isolate the hftb/teed complex $\text{Cu}(\text{hftb})_2(\text{teed})$; no reaction occurs upon treatment of copper(II) methoxide with hftbH and teed in diethyl ether, and only decomposition products were generated in refluxing benzene.

The pyridine complexes **5** and **8** can be prepared in higher yields by treating CuBr_2 with the sodium salts $\text{Na}(\text{hfip})$ or $\text{Na}(\text{hftb})$ in tetrahydrofuran followed by removal of the solvent and addition of pyridine in pentane.



Attempts were made to prepare analogues of the above complexes with *tert*-butoxide groups in place of the fluoroalkoxide ligands, but no evidence was seen for the formation of a soluble $\text{Cu}(\text{O}-t\text{-Bu})_2(\text{L})_2$ species. Also, attempts to prepare hfip and hftb complexes with trimethylamine or triethylamine as the Lewis bases were unsuccessful.

The physical and microanalytical data for compounds **1–8** are given in Table I. Compounds **2–8** are soluble in benzene, toluene, diethyl ether, tetrahydrofuran, and CH_2Cl_2 ; the pyridine complexes **5** and **8** are also soluble in pentane. Interestingly, the tmed compound $\text{Cu}(\text{hfip})_2(\text{tmed})$ (**2**) can be dissolved in water and stirred in solution for long periods without decomposition. However, if these aqueous solutions of **2** are refluxed, copper(II) oxide, CuO , is formed.

All of these fluoroalkoxide complexes except the pyridine derivatives should adopt *cis* square-planar geometries due to the chelating nature of the amine ligands. In contrast, the pyridine derivatives **5** and **8** presumably adopt *trans* square-planar structures like that present in the related siloxide complex $\text{trans-Cu}[\text{OSi}(\text{O}-t\text{-Bu})_3]_2(\text{py})_2$.¹⁷

Molecular Structures of $\text{Cu}(\text{hfip})_2(\text{tmed})$ (2**) and $\text{Cu}(\text{hftb})_2(\text{tmed})$ (**6**).** The molecular structures of **2** and **6** are of interest because these are rare examples of monomeric copper(II) complexes with unidentate alkoxide ligands. The ORTEP diagrams are shown in Figures 1 and 2, crystal data are collected in Table II, final atomic coordinates are given in Table III and IV, and selected bond distances and angles are presented in Tables V and VI.

Although molecules of **2** reside on general positions within the unit cell, molecules of **6** lie on crystallographic 2-fold axes that bisect the O–Cu–O and N–Cu–N angles. Both compounds assume somewhat distorted square-planar geometries. The average Cu–O distances of 1.903 (3) Å in **2** and 1.884 (3) Å in **6** are similar to those reported for several other copper(II) alkoxide complexes: 1.848 (5) Å in $\text{Cu}[\text{OSi}(\text{O}-t\text{-Bu})_3]_2(\text{py})_2$,¹⁷ 1.865 (3) Å in $\text{Cu}[\text{O}(\text{CH}_2)_2\text{NMe}_2]_2$,¹⁰ 1.90 (2) Å in $\text{Cu}[\text{OCHPhCHMeNHMe}]_2$,¹⁸ 1.878 (7) Å in $\text{Ba}[\text{Cu}(\text{hftb})_3]_2$,¹² 1.89 (2) Å in $\text{Cu}[\text{O}(\text{CH}_2)_2\text{NMe}(\text{CH}_2)_2\text{NMe}_2]_2$,¹⁰ and 1.916 (5) Å in $\text{Na}_2[\text{Cu}(\text{hfip})_4]$.¹³ The average Cu–N distances of 2.035 (5) Å in **2** and 2.064 (3) Å in **6** are also similar to those in related molecules: 2.000 (3) Å in $\text{Cu}(\text{tmed})(\text{NO}_3)_2$,¹⁹ 2.029 (5) Å in $[\text{Cu}(\text{OPh})_2(\text{H}_2\text{N}(\text{CH}_2)_2\text{NH}_2)]_2 \cdot 2\text{PhOH}$,²⁰ 2.031 (5) Å in $[\text{Cu}(\text{tmed})(\text{N-methylformamide})_3](\text{ClO}_4)_2$,²¹ 2.052 (3) Å in $\text{Cu}[\text{O}(\text{CH}_2)_2\text{NMe}_2]_2$,¹⁰ 2.02 (2) Å in $\text{Cu}[\text{OCHPhCHMeNHMe}]_2$,¹⁸ and 2.11 (1) Å in $\text{Cu}[\text{O}(\text{CH}_2)_2\text{NMe}(\text{CH}_2)_2\text{NMe}_2]_2$.¹⁰ The relatively small Cu–O–C angles of 116.1 (3) and 120.9 (3)° in **2** and 125.5 (2)° in **6** indicate that π bonding between the alkoxide ligands and the copper centers is relatively unimportant, as expected for a d^9 metal.

Both molecules are distorted in several ways from perfect square-planar geometries. First, the chelating nature of the tmed ligands causes the N–Cu–N angles of 85.8° in **2** and 85.2° in **6** to be smaller than the ideal value of 90°. Second, the large steric bulk of the alkoxide ligands is reflected in the relatively large O–Cu–O angles of 96.4 (2)° in **2** and 105.5 (1)° in **6**. Third, the dihedral angle between the CuN_2 and CuO_2 planes is not zero as would be expected for an ideal square-planar structure: these dihedral angles are 16.1° for **2** and 40.6° for **6**. These tetrahedral distortions are shown in Figure 3, where both complexes are viewed down the axis that bisects the O–Cu–O and N–Cu–N angles. Without doubt, the larger steric bulk of hftb ligands vs hfip ligands is responsible for the larger O–Cu–O angle, the larger tetrahedral distortion from square-planar geometry, and the larger Cu–O–C angle in compound **6**.

There are several H...F nonbonded contacts that are worth noting in these molecules. In **2** there are three intramolecular contacts that are under 2.50 Å: $\text{H1}\cdots\text{F2c} = 2.47$ (5) Å, $\text{H1}\cdots\text{F3b} = 2.44$ (5) Å, and $\text{H1}\cdots\text{F3c} = 2.44$ (5) Å; in **6** there are two short intramolecular contacts, $\text{H7c}\cdots\text{F3} = 2.55$ (5) Å and $\text{H7c}\cdots\text{F3}' = 2.51$ (4) Å, and one short intermolecular contact, $\text{H1a}\cdots\text{F3}' = 2.51$ (4) Å. For comparison, the sum of the van der Waals radii of hydrogen and fluorine is 2.55 Å, and hydrogen-bonding interactions involving fluorine atoms are typically 2.25–2.8 Å in species such as crystalline HF, salts of the HF_2^- anion, and related

(17) McMullen, A. K.; Tilley, T. D.; Rheingold, A. L.; Geib, S. J. *Inorg. Chem.* **1989**, *28*, 3772–3774.

(18) Bailey, N. A.; Harrison, P. M.; Mason, R. J. *Chem. Soc., Chem. Commun.* **1968**, 559–560.

(19) Gomez de Anderez, D.; Mukherjee, A. K.; Koner, S.; Chaudhuri, N. R. *Polyhedron* **1991**, *10*, 2225–2227.

(20) Calderazzo, F.; Marchetti, F.; Dell'Amico, G.; Pelizzi, G.; Colligiani, A. J. *Chem. Soc., Dalton Trans.* **1980**, 1419–1424.

(21) Su, C. C.; Tsai, H. L.; Li, S. R.; Wang, S. L.; Cheng, C. Y. *Transition Met. Chem. (London)* **1990**, *15*, 454–458.

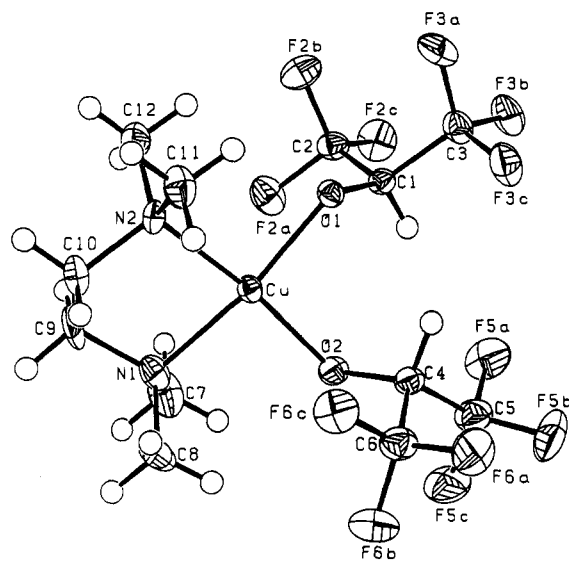
Table I. Physical and Microanalytical Data for Compounds 1-8

cmpd	color	mp, °C	% calcd				% found			
			C	H	N	Cu	C	H	N	Cu
Cu(hfip)(OMe) (1)	turquoise		19.7	1.65		26.1	17.2	1.78		26.6
Cu(hfip) ₂ (tmed) (2)	purple	105-108	28.1	3.16	5.47	12.4	28.4	3.52	5.60	12.7
Cu(hfip) ₂ (teed) (3)	purple	97-100	33.7	4.60	4.92	11.2	34.0	4.70	5.06	11.2
Cu(hfip) ₂ (bipy) (4)	purple	150 dec	34.7	1.82	5.06	11.5	34.9	1.84	5.11	11.6
Cu(hfip) ₂ (py) ₂ (5)	purple	63-66	34.6	2.18	5.04	11.4	34.5	2.26	5.06	11.2
Cu(hftb) ₂ (tmed) (6)	blue	136-138	31.0	4.10	5.16	11.7	31.0	4.14	5.10	11.9
Cu(hftb) ₂ (bipy) (7)	purple	150 dec	37.2	2.43	4.81	10.9	37.2	2.42	4.76	11.1
Cu(hftb) ₂ (py) ₂ (8)	turquoise	70-72	37.0	2.76	4.80	10.9	36.9	3.00	4.74	10.7

Table II. Crystallographic Data for Cu(hfip)₂(tmed) (2) and Cu(hftb)₂(tmed) (6)

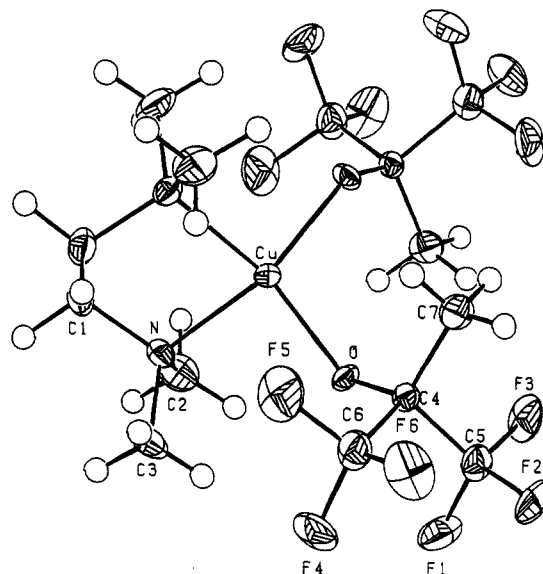
	2	6
formula	C ₁₂ H ₁₈ CuF ₁₂ N ₂ O ₂	C ₁₄ H ₂₂ CuF ₁₂ N ₂ O ₂
mol wt	513.82	541.87
space gp	P2 ₁ /c	I2/a
T, °C	-75	-75
a, Å	9.454 (1)	13.601 (3)
b, Å	15.045 (2)	9.567 (2)
c, Å	14.197 (6)	16.562 (5)
β, °	105.65 (2)	106.56 (2)
V, Å ³	1944 (1)	2066 (2)
Z	4	4
λ, Å	0.710 73	0.710 73
ρ _{calcd} , g cm ⁻³	1.756	1.742
μ _{calcd} , cm ⁻¹	12.43	11.74
transm factors	0.697-0.646	0.881-0.738
R ^a	0.040	0.043
R _w ^b	0.052	0.037

$${}^a R = \sum(|F_o| - |F_c|) / \sum|F_o|, {}^b R_w = (\sum w(|F_o| - |F_c|)^2 / \sum w|F_o|^2)^{1/2}.$$

Figure 1. ORTEP diagram of Cu(hfip)₂(tmed) (2). Thermal ellipsoids are drawn at the 35% probability level.

compounds.²² In these copper complexes, no special significance is ascribed to the H...F contacts that are present, since the hydrogen atoms involved are all bonded to carbon and are not expected to be particularly prone to formation of hydrogen bonds.

Spectroscopic Studies of the Copper(II) Fluoroalkoxide Complexes. The EPR spectra of 2-8 have been recorded in toluene solutions at 273 K and in toluene glasses at 120 K (Table VII). Although all of the spectra are of the rhombic type, with g_z lying between 2.23 and 2.34 and g_x and g_y lying between 1.99 and 2.07, the degree of rhombic splitting is small and the spectra closely resemble those characteristic of axially symmetric species (Figure 4). Hyperfine coupling due to the ⁶³Cu and ⁶⁵Cu nuclear spins

Figure 2. ORTEP diagram of Cu(hftb)₂(tmed) (6). Thermal ellipsoids are drawn at the 35% probability level.Table III. Final Atomic Coordinates for Cu(hfip)₂(tmed) (2)

	x/a	y/b	z/c
Cu	0.79563 (7)	0.83660 (4)	0.14449 (5)
O1	0.7261 (4)	0.8882 (2)	0.2466 (3)
O2	0.9848 (4)	0.8891 (3)	0.1818 (3)
N1	0.8324 (6)	0.7967 (3)	0.0161 (3)
N2	0.6180 (5)	0.7547 (3)	0.1086 (3)
C1	0.7426 (6)	0.9785 (4)	0.2580 (4)
C2	0.6331 (6)	1.0285 (4)	0.1780 (4)
F2a	0.6488 (4)	1.0028 (2)	0.0906 (2)
F2b	0.4944 (4)	1.0140 (3)	0.1750 (3)
F2c	0.6530 (4)	1.1163 (2)	0.1826 (3)
C3	0.7326 (6)	1.0041 (4)	0.3596 (4)
F3a	0.6052 (4)	0.9810 (3)	0.3764 (3)
F3b	0.7494 (4)	1.0918 (2)	0.3764 (3)
F3c	0.8369 (4)	0.9643 (2)	0.4279 (3)
C4	1.0673 (6)	0.8862 (4)	0.2755 (4)
C5	1.1735 (7)	0.9652 (5)	0.2946 (5)
F5a	1.1001 (4)	1.0413 (3)	0.2885 (3)
F5b	1.2690 (5)	0.9630 (3)	0.3843 (3)
F5c	1.2532 (4)	0.9699 (3)	0.2322 (3)
C6	1.1498 (7)	0.7966 (5)	0.2966 (5)
F6a	1.2239 (4)	0.7884 (3)	0.3899 (3)
F6b	1.2454 (4)	0.7857 (3)	0.2430 (3)
F6c	1.0546 (4)	0.7306 (2)	0.2763 (3)
C7	0.8634 (9)	0.8763 (5)	-0.0382 (5)
C8	0.9587 (7)	0.7358 (5)	0.0330 (5)
C9	0.6966 (7)	0.7518 (5)	-0.0406 (4)
C10	0.6362 (7)	0.6972 (4)	0.0276 (4)
C11	0.6130 (7)	0.6987 (4)	0.1933 (5)
C12	0.4791 (7)	0.8050 (4)	0.0785 (5)
H1	0.831 (6)	1.000 (3)	0.259 (4)
H4	1.002 (5)	0.893 (3)	0.320 (4)

($I = 3/2$) is apparent in all of the 120 K spectra, with the A_z couplings being large and lying between 0.0102 and 0.0203 cm⁻¹. As is often the case in near-axial copper(II) EPR spectra, the A_x and A_y hyperfine couplings are too small to resolve. Superhy-

(22) Pauling, L. *The Nature of the Chemical Bond*, 3rd ed.; Cornell University Press: Ithaca, NY, 1960; Chapter 12-3.

Table IV. Final Atomic Coordinates for Cu(hfip)₂(tmed) (6)

	<i>x/a</i>	<i>y/b</i>	<i>z/c</i>
Cu	0.2500	0.35156 (8)	0.0000
F1	0.4869 (2)	0.6230 (3)	0.1822 (2)
F2	0.3824 (2)	0.7465 (3)	0.2265 (2)
F3	0.3820 (2)	0.7587 (3)	0.0970 (2)
F4	0.4057 (2)	0.4145 (3)	0.2533 (2)
F5	0.2508 (2)	0.3555 (3)	0.1917 (2)
F6	0.2820 (2)	0.5334 (3)	0.2735 (2)
O	0.3383 (2)	0.4708 (3)	0.0787 (2)
N	0.3571 (3)	0.1927 (3)	0.0240 (2)
C1	0.3004 (4)	0.0646 (5)	-0.0101 (3)
C2	0.4332 (4)	0.2277 (7)	-0.0202 (4)
C3	0.4120 (5)	0.1742 (7)	0.1147 (3)
C4	0.3105 (3)	0.5531 (4)	0.1358 (2)
C5	0.3910 (3)	0.6698 (5)	0.1614 (3)
C6	0.3137 (4)	0.4657 (5)	0.2146 (3)
C7	0.2048 (4)	0.6198 (6)	0.1056 (3)
H1a	0.343 (3)	-0.021 (4)	0.012 (2)
H1b	0.285 (3)	0.064 (4)	-0.069 (3)
H2a	0.470 (3)	0.324 (5)	-0.004 (2)
H2b	0.399 (3)	0.233 (5)	-0.076 (3)
H2c	0.485 (4)	0.165 (6)	-0.016 (3)
H3a	0.358 (3)	0.156 (5)	0.145 (3)
H3b	0.462 (3)	0.104 (4)	0.119 (3)
H3c	0.451 (4)	0.258 (6)	0.133 (3)
H7a	0.187 (3)	0.679 (5)	0.141 (3)
H7b	0.155 (4)	0.551 (5)	0.102 (3)
H7c	0.196 (3)	0.677 (5)	0.052 (3)

Table V. Selected Bond Distances (Å) and Angles (deg) for Cu(hfip)₂(tmed) (2)

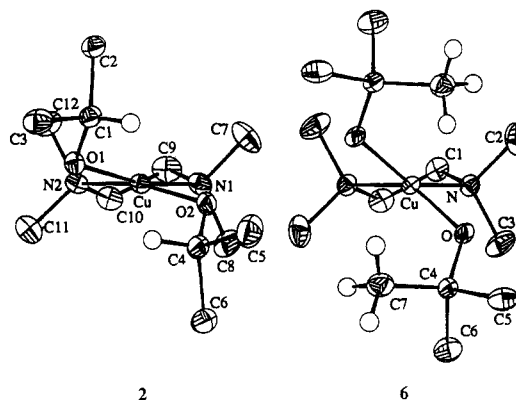
Bond Distances			
Cu-O1	1.910 (3)	Cu-O2	1.895 (4)
Cu-N1	2.036 (5)	Cu-N2	2.034 (4)
C4-O2	1.349 (7)	C1-O1	1.372 (6)
C4-H4	1.00 (5)	C1-H1	0.90 (5)
C4-C5	1.531 (9)	C1-C2	1.514 (8)
C4-C6	1.546 (9)	C1-C3	1.520 (8)
N1-C7	1.495 (8)	N1-C8	1.472 (8)
N1-C9	1.482 (8)	N2-C10	1.485 (7)
N2-C11	1.479 (8)	N2-C12	1.475 (7)
C9-C10	1.495 (9)		
Bond Angles			
O1-Cu-O2	96.4 (2)	N1-Cu-N2	85.8 (2)
O1-Cu-N2	90.3 (2)	O2-Cu-N1	89.8 (2)
O1-Cu-N1	167.4 (2)	O2-Cu-N2	167.3 (2)
Cu-O1-C1	116.1 (3)	Cu-O2-C4	120.9 (3)
O1-C1-H1	116 (3)	O2-C4-H4	109 (3)
O1-C1-C2	111.8 (4)	O2-C4-C5	109.1 (5)
O1-C1-C3	109.2 (4)	O2-C4-C6	110.2 (5)

Table VI. Selected Bond Distances (Å) and Angles (deg) for Cu(hftb)₂(tmed) (6)

Bond Distances			
Cu-O	1.884 (3)	Cu-N	2.064 (3)
N-C1	1.473 (6)	N-C2	1.466 (7)
N-C3	1.485 (6)	O-C4	1.364 (5)
C4-C5	1.536 (6)	C4-C6	1.541 (6)
C4-C7	1.521 (6)	C1-C1'	1.500 (7)
Bond Angles			
O-Cu-O'	105.5 (1)	N-Cu-N'	85.2 (1)
O-Cu-N	148.7 (1)	O-Cu-N	92.1 (1)
Cu-O-C4	125.5 (2)	O-C4-C5	107.2 (3)
O-C4-C6	109.1 (3)	O-C4-C7	116.0 (3)

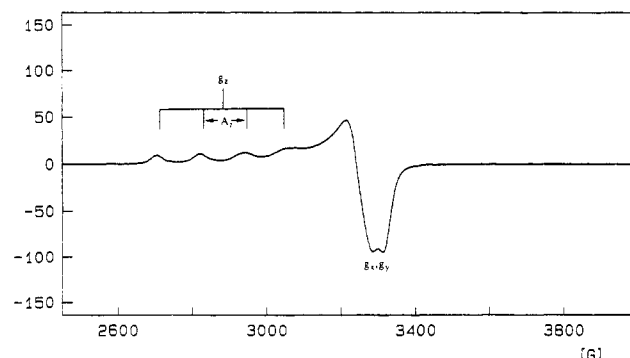
perfine couplings to ligand nuclei are seen only in the spectra of the py and bipy complexes: in both cases, the "A_⊥" splittings of approximately 0.0019 cm⁻¹ are probably due to hydrogen nuclei on the amine ligands.

It has been shown previously that *g_z* increases and the hyperfine coupling *A_z* decreases as the distortion from square-planar geometry in copper(II) complexes becomes more pronounced.²³⁻²⁷ In the fluoroalkoxide complexes, the values of *g_z* and *A_z* are in fact correlated, and the data suggest that the degree of distortion

**Figure 3.** Structures of Cu(hfip)₂(tmed) (2) and Cu(hftb)₂(tmed) (6) illustrating their tetrahedral distortions from ideal square-planar geometries. The fluorine atoms have been omitted for clarity. The dihedral angles between the CuN₂ and CuO₂ planes are 16.1° for 2 and 40.6° for 6.**Table VII.** EPR Data for Compounds 2-8 in toluene^a

cmpd	glass (120 K)			soln (273 K)	
	<i>g_z</i>	<i>g_x, g_y</i>	<i>A_z</i> ^b	<i>g</i>	<i>A</i> ^b
Cu(hfip) ₂ (bipy) (4)	2.23	2.03, 1.99	205	2.12	87
Cu(hfip) ₂ (tmed) (2)	2.24	2.03, 1.99	186	2.11	81
Cu(hfip) ₂ (teed) (3)	2.24	2.03, 2.00	184	2.13	80
Cu(hftb) ₂ (bipy) (7)	2.28	2.06, 2.01	169	2.14	70
Cu(hfip) ₂ (py) ₂ (5)	2.28	2.05, 2.01	165	2.13	60
Cu(hftb) ₂ (tmed) (6)	2.33	2.04, 2.03	132	2.14	<i>d</i>
Cu(hftb) ₂ (py) ₂ (8)	2.34	2.07 ^c	105	2.18	<i>d</i>

^a Compounds are listed in order of increasing tetrahedral distortion. ^b 10⁻⁴ cm⁻¹. ^c Three smaller peaks at lower *g* values may arise from rhombic splitting or from small amounts of impurities in the sample. ^d Not discernible.

**Figure 4.** X-Band EPR spectrum of Cu(hftb)₂(tmed) (6) in a toluene glass at 120 K.

from a square-planar geometry increases in the order 4 < 2 < 3 < 7 < 5 < 6 < 8.²⁸ This order is consistent with the expected relative steric requirements of the ligands: hfip < hftb, and bipy < tmed < teed < (py)₂.

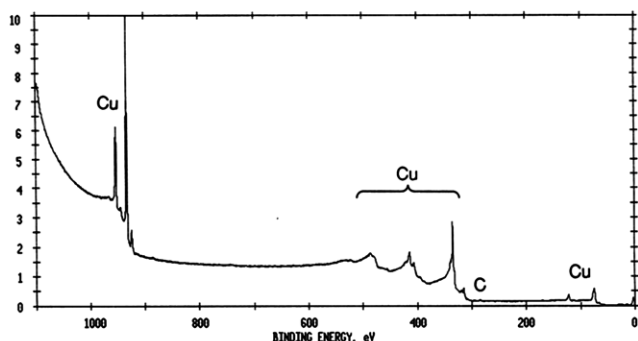
The electronic absorption spectra of compounds 2-8 have been recorded in CH₂Cl₂ solutions at room temperature, and the results are shown in Table VIII. The energies of the d-d transitions in

- (23) Peisach, J.; Blumberg, W. E. *Arch. Biochem. Biophys.* **1974**, *165*, 691-708.
- (24) Hathaway, B. J. In *Comprehensive Coordination Chemistry*; Wilkinson, G., Ed.; Pergamon Press, Oxford, U.K., 1987; Vol. 5, pp 662-673.
- (25) Yokoi, H.; Addison, A. W. *Inorg. Chem.* **1977**, *16*, 1341-1349.
- (26) Yokoi, H. *Bull. Chem. Soc. Jpn.* **1974**, *47*, 3037-3040.
- (27) Murakami, Y.; Matsuda, Y.; Sakata, K. *Inorg. Chem.* **1971**, *10*, 1734-1738.
- (28) This series contains both compounds with cis geometries 2, 3, 4, 6, and 7, and compounds probably with trans geometries 5 and 8, and therefore caution must be exercised in drawing conclusions about the relative degrees of tetrahedral distortions in compounds 2-8, since the effect of trans vs cis geometry on *g_z*, *A_z*, and the d-d transition energies is not known; the fact that 5 and 8 fall correctly in the series may be coincidental.

Table VIII. Electronic Spectral Data for Compounds 2–8 in CH₂Cl₂ Solution at Room Temperature^a

compd	λ_{\max} , nm	ϵ , cm ⁻¹ M ⁻¹	λ_{\max} , nm	ϵ , cm ⁻¹ M ⁻¹	
Cu(hfip) ₂ (bipy) (4)	548	157	Cu(hfip) ₂ (py) ₂ (5)	628	96
Cu(hfip) ₂ (tmed) (2)	576	347	Cu(hftb) ₂ (tmed) (6)	656	200
Cu(hfip) ₂ (teed) (3)	598	186	Cu(hftb) ₂ (py) ₂ (8)	680	105
Cu(hftb) ₂ (bipy) (7)	600	155			

^a Compounds are listed in order of increasing tetrahedral distortion.

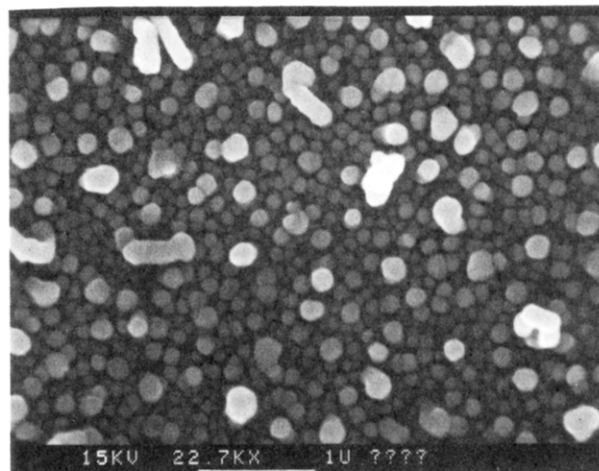
**Figure 5.** X-ray photoelectron spectrum of copper metal deposit produced by MOCVD of 2 at 300 °C.

copper(II) complexes can also serve as indicators of the amount of distortion from an ideal square-planar geometry.^{24,25,29–31} As a copper(II) complex becomes more tetrahedrally distorted, the $d_{x^2-y^2}$ orbital becomes less antibonding and thus the $d \rightarrow d_{x^2-y^2}$ transitions occur at lower energies. Reassuringly, the ranking of compounds 2–8 in order of increasing distortion from a square-planar geometry as deduced from the electronic absorption spectra is the same as that obtained from the EPR data. Good correlations between the $d-d$ transition energies and the EPR parameters g_z and A_z have been noted previously for copper(II) complexes.^{25,26}

Metal–Organic Chemical Vapor Deposition Studies. Several of the new fluoroalkoxide complexes described above are volatile: compounds 2, 3, 4, and 6 sublime readily at 75 °C and 10⁻⁵ Torr, and compound 7 sublimates at 140 °C and 10⁻⁵ Torr.³² In contrast, the pyridine complexes 5 and 8 lose pyridine readily and decompose rather than sublime when heated to 70 °C under vacuum. Since Cu(hfip)₂(tmed) (2) is reasonably volatile and serves as a representative example of the fluoroalkoxide complexes, it was chosen for further study as a MOCVD precursor.

A reservoir of 2 was maintained at 70 °C, and the resulting vapor was passed over silicon wafers heated to 300 °C, which is the lowest temperature at which deposition will occur. The X-ray photoelectron spectrum (Figure 5) shows that the deposits consist of ca. 99% pure copper metal; oxygen, nitrogen, and fluorine are not present to detectable levels in the deposits, but a small amount of carbon (~1%) is present. The deposits do not diffract X-rays coherently and so may be regarded as amorphous. Scanning electron micrographs (Figure 6) show that the deposits consist of small granules that are roughly 0.1–0.4 μm in diameter.

Thus, in the absence of water and oxygen, these new copper(II) fluoroalkoxide complexes serve as MOCVD precursors to copper metal rather than copper oxide phases. This seems to be a general pattern, since similar behavior is observed for other

**Figure 6.** Scanning electron micrograph of copper metal deposit produced by MOCVD from Cu(hfip)₂(tmed) (2) showing 0.1–0.4-μm particles.

copper(II) MOCVD precursors.^{14,33–37} This behavior can be understood since we have described previously that copper oxides readily deoxygenate under vacuum at temperatures as low as 300 °C.⁵ At these temperatures, the presence of a carrier gas that contains oxygen is therefore necessary to prevent deoxygenation and to grow copper oxide phases from MOCVD precursors.

Although Cu(hfip)₂(tmed) (2) does deposit copper metal films under MOCVD conditions, our results suggest that it is not likely to replace other copper complexes, particularly copper β-diketetonates, as a CVD precursor to copper metal. Specifically, it is less volatile than copper(I) and copper(II) complexes with fluorinated β-diketetonate ligands and does not sublime quantitatively. Nevertheless, the fluoroalkoxide complexes are the first examples of a new class of volatile copper-containing molecules, and it is possible that other representatives of this class may prove to be more attractive as MOCVD precursors.

Concluding Remarks. The first electrically neutral copper(II) complexes that contain unidentate fluoroalkoxide ligands have been prepared and have been shown to adopt tetrahedrally-distorted square-planar geometries in the solid state. The degree of distortion has been probed by EPR and UV–vis spectroscopy and by X-ray crystallography and has been shown to increase as the ligands become larger. The fluoroalkoxide complexes are slow to hydrolyze, and some of them are volatile and can serve as MOCVD precursors to copper metal films at 300 °C and 10⁻⁵ Torr.

Experimental Section

All operations were carried out under vacuum or under argon. Solvents were distilled under nitrogen from sodium (toluene), sodium benzophenone (diethyl ether, benzene, pentane, and tetrahydrofuran), or CaH₂ (dichloromethane) immediately before use. The fluoroalcohols 1,1,1,3,3,3-hexafluoro-2-propanol and 1,1,1,3,3,3-hexafluoro-2-methyl-2-propanol (PCR) were distilled from Linde 3A molecular sieves, *N,N,N',N'*-tetramethylethylenediamine, *N,N,N',N'*-tetraethylethylenediamine, and pyridine (Aldrich) were distilled from sodium, and 2,2'-bipyridine (Aldrich) was recrystallized from pentane. [Cu(OMe)₂]_n was prepared by a literature route.³⁸ Na(hfip) was prepared by the dropwise addition of the alcohol to sodium in diethyl ether; after 4 h, the solvent was removed and the residue was dried under vacuum at 100 °C and crystallized from hot toluene. Na(hftb) was prepared similarly in tetrahydrofuran and was purified by sublimation at 110 °C under vacuum. Silicon (100)

(29) Hathaway, B. J. In *Comprehensive Coordination Chemistry*; Wilkinson, G., Ed.; Pergamon: Oxford, U.K., 1987; Vol. 5, pp 674–679.

(30) Tomlinson, A. A. G.; Hathaway, B. J.; Billing, D. E.; Nichols, P. J. *Chem. Soc. A* 1969, 65–71.

(31) Murakami, Y.; Matsuda, Y.; Sakata, K. *Inorg. Chem.* 1971, 10, 1728–1734.

(32) The sublimates obtained from the bipyridine complexes 4 and 7 are contaminated with free bipy because of partial decomposition. In addition, the sublimation yields for 2, 3, and 6 are not quantitative because the compounds partially convert at 75 °C to nonvolatile oils. Interestingly, the microanalytical data suggest that these oils have the same composition as their molecular precursors.

(33) Kaloyeros, A. E.; Feng, A.; Garhart, J.; Brooks, K.; Ghosh, S.; Saxena, A.; Luehrs, F. J. *Electron. Mater.* 1990, 19, 271–276.

(34) Temple, D.; Reisman, A. J. *Electrochem. Soc.* 1989, 136, 3525–3529.

(35) Kaloyeros, A. E.; Saxena, A. N.; Brooks, K.; Ghosh, S.; Einsenbraun, E. *Mater. Res. Soc. Symp. Proc.* 1990, 181, 79–85.

(36) Armitage, D. N.; Dunhill, N. I.; West, R. H.; Williams, J. O. *J. Cryst. Growth* 1991, 108, 683–687.

(37) Pauleau, Y.; Fasasi, A. Y. *Chem. Mater.* 1991, 3, 45–50.

(38) Brubaker, C. H.; Wicholas, M. J. *Inorg. Nucl. Chem.* 1965, 27, 59–62.

wafers, n-doped, 0.38 mm thick, were obtained from Monsanto and were cut to 1.5 × 1.5 mm squares.

X-ray photoelectron spectra were induced by a 15-kV, 400-W Mg K α radiation source (1253.6 eV) on a Perkin-Elmer 5400 ESCA/Auger system with a pass energy of 89.45 eV and an energy resolution of 0.5 eV/step. The samples were argon-sputtered to remove surface contamination before spectra were obtained. X-ray diffraction data were recorded on a Rigaku D-Max powder diffractometer. Scanning electron micrographs were obtained on a ISI DS-130 instrument. The ^1H NMR data were recorded on a General Electric GN-300 NB spectrometer at 300 MHz. The X-band EPR data were recorded on a Bruker ESP 300 spectrometer. IR spectra were recorded on a Perkin-Elmer 599B infrared spectrometer as Nujol mulls. UV-vis spectra were recorded on a Hewlett-Packard 8452A diode array spectrometer. Microanalyses were performed by the University of Illinois Microanalytical Laboratory.

(1,1,1,3,3,3-Hexafluoro-2-propoxo)(methoxo)copper(II) (1). To a suspension of $[\text{Cu}(\text{OMe})_2]_n$ (0.98 g, 7.8 mmol) in benzene (20 mL) at room temperature was added 1,1,1,3,3,3-hexafluoro-2-propanol (10 mL, 95 mmol). The solution was refluxed for 4 h. The resulting turquoise-colored solid was collected by filtration and dried under vacuum. Yield: 1.02 g (50%). IR (cm^{-1}): 1357 m, 1285 s, 1259 s, 1198 vs, 1168 s, 1143 m, 1127 s, 1096 s, 1050 m, 1035 sh, 891 m, 855 s, 742 m, 690 m, 637 w, 534 s, 442 w.

Bis(1,1,1,3,3,3-hexafluoro-2-propoxo)(*N,N,N',N'*-tetramethylethylenediamine)copper(II) (2). **Method 1.** To a suspension of $[\text{Cu}(\text{OMe})_2]_n$ (0.25 g, 2.0 mmol) in diethyl ether (10 mL) at room temperature were added *N,N,N',N'*-tetramethylethylenediamine (1.25 mL, 8.3 mmol) and 1,1,1,3,3,3-hexafluoro-2-propanol (0.5 mL, 4.7 mmol). The solution immediately turned dark purple. After being stirred for 30 min, the solution was filtered, and the filtrate was concentrated to ca. 5 mL and cooled to -20°C to yield dark purple crystals. Additional crops of crystals were obtained by further concentration and cooling of the supernatant. Yield: 0.80 g (78%). IR (cm^{-1}): 1351 s, 1284 vs, 1270 vs, 1175 vs, 1082 s, 1049 m, 1023 m, 1008 m, 958 m, 890 s, 850 s, 812 s, 771 m, 744 s, 691 s, 540 sh, 531 m, 453 w, 430 w.

Method 2. To **1** (0.20 g, 2.0 mmol) was added *N,N,N',N'*-tetramethylethylenediamine (10 mL, 66 mmol). The solution immediately turned dark purple. It was then filtered, and the filtrate was concentrated to ca. 7 mL and cooled to -20°C to yield dark purple crystals. Yield: 0.14 g (36%).

Bis(1,1,1,3,3,3-hexafluoro-2-propoxo)(*N,N,N',N'*-tetraethylethylenediamine)copper(II) (3). To a suspension of $[\text{Cu}(\text{OMe})_2]_n$ (0.20 g, 1.6 mmol) in diethyl ether (20 mL) at room temperature were added *N,N,N',N'*-tetraethylethylenediamine (1.0 mL, 4.7 mmol) and 1,1,1,3,3,3-hexafluoro-2-propanol (0.5 mL, 4.7 mmol). The solution immediately turned purple. After being stirred for 30 min, the solution was filtered, and the filtrate was concentrated to ca. 10 mL and cooled to -20°C to yield dark purple crystals. Yield: 0.70 g (77%). IR (cm^{-1}): 1485 m, 1397 s, 1365 s, 1352 s, 1332 s, 1270 vs, 1170 vs, 1087 vs, 1057 s, 1039 m, 999 m, 919 w, 904 w, 879 s, 850 s, 811 w, 799 w, 765 m, 743 m, 687 s, 578 m, 526 m. ^1H NMR (C_7D_8 , 293 K): δ -0.31 (s, fwhm 480 Hz, NCH_2CH_3).

Bis(1,1,1,3,3,3-hexafluoro-2-propoxo)(2,2'-bipyridine)copper(II) (4). To a suspension of $[\text{Cu}(\text{OMe})_2]_n$ (0.5 g, 4.0 mmol) in diethyl ether (20 mL) were added 2,2'-bipyridine (0.62 g, 4.0 mmol) and 1,1,1,3,3,3-hexafluoro-2-propanol (0.75 mL, 7.1 mmol) at room temperature. The solution turned purple immediately. After being stirred for 30 min the solution was filtered, and the filtrate was concentrated to ca. 10 mL and cooled to -20°C to yield purple needles. Additional crops of crystals were obtained by further concentration and cooling of the supernatant. Yield: 1.85 g (84%). IR (cm^{-1}): 1621 m, 1613 m, 1585 w, 1577 w, 1500 w, 1480 m, 1385 m, 1359 m, 1319 m, 1283 s, 1262 s, 1190 vs, 1115 m, 1092 s, 1064 m, 1048 w, 1039 m, 1023 w, 1015 sh, 997 w, 890 m, 851 s, 775 s, 749 m, 739 m, 691 s, 668 w, 658 vw, 640 w, 542 w, 519 w, 430 w. ^1H NMR (C_7D_8 , 298 K): δ 9.20 (s, fwhm 310 Hz, $\text{C}_{10}\text{N}_2\text{H}_8$).

Bis(1,1,1,3,3,3-hexafluoro-2-propoxo)bis(pyridine)copper(II) (5). **Method 1.** To a suspension of $[\text{Cu}(\text{OMe})_2]_n$ (0.5 g, 4.0 mmol) in diethyl ether (20 mL) at room temperature were added pyridine (0.64 mL, 7.9 mmol) and 1,1,1,3,3,3-hexafluoro-2-propanol (1.0 mL, 9.5 mmol). The solution was stirred for 4 h and filtered, and the solvent was removed under vacuum. The residue was dried under vacuum overnight to yield a purple solid and some green oil. The residue was extracted with pentane (100 mL), and the filtered extract was concentrated to ca. 20 mL and cooled to -72°C to yield a purple powder. Yield: 0.45 g (20%). IR (cm^{-1}): 1610 m, 1601 m, 1485 m, 1286 s, 1260 s, 1181 vs, 1095 s, 1071 s, 1047 m, 1017 m, 960

m, 889 s, 847 s, 798 m, 757 s, 740 s, 700 s, 686 s, 642 m, 526 m, 435 m. ^1H NMR (C_7D_8 , 298 K): δ 13.21 (s, fwhm 410 Hz, para CH).

Method 2. To a suspension of CuBr_2 (0.5 g, 2.2 mmol) in tetrahydrofuran (100 mL) was added sodium 1,1,1,3,3,3-hexafluoro-2-propoxide (0.85 g, 4.4 mmol). After being stirred for 3 h, the solution turned green and a white precipitate formed. The solvent was removed under vacuum, and the residue was treated with pentane (100 mL) and pyridine (0.36 mL, 4.4 mmol). After being stirred for 30 min, the resulting blue solution was filtered, and the filtrate was concentrated to ca. 30 mL and cooled to -20°C to yield blue crystals. Yield: 0.38 g (31%).

Bis(1,1,1,3,3,3-hexafluoro-2-methyl-2-propoxo)(*N,N,N',N'*-tetramethylethylenediamine)copper(II) (6). To a suspension of $[\text{Cu}(\text{OMe})_2]_n$ (0.5 g, 4.0 mmol) in benzene (20 mL) at room temperature were added *N,N,N',N'*-tetramethylethylenediamine (5 mL, 33 mmol) and 1,1,1,3,3,3-hexafluoro-2-methyl-2-propanol (1.0 mL, 8.0 mmol). After being refluxed for 2 h, the solution turned dark blue. The solution was filtered, and the residue was extracted with benzene (2×20 mL). The filtrate and filtered extracts were combined, and the solvent was removed under vacuum. The residue was extracted with diethyl ether (50 mL), the resulting solution was filtered, and the filtrate was concentrated to ca. 10 mL and cooled to -20°C to yield blue crystals. Additional crops of crystals were obtained by further concentration and cooling of the supernatant. Yield: 0.74 g (34%). IR (cm^{-1}): 1411 w, 1354 w, 1309 s, 1292 s, 1213 vs, 1171 vs, 1113 s, 1070 s, 1043 m, 1028 m, 1010 m, 960 s, 856 m, 810 m, 770 w, 759 w, 703 s, 653 vw, 626 m, 536 m, 510 w, 474 vw, 455 vw. ^1H NMR (C_7D_8 , 298 K): δ -5.27 (s, fwhm 450 Hz, $\text{O}(\text{CH}_3)(\text{CF}_3)_2$).

Bis(1,1,1,3,3,3-hexafluoro-2-methyl-2-propoxo)(2,2'-bipyridine)copper(II) (7). To a suspension of $[\text{Cu}(\text{OMe})_2]_n$ (0.25 g, 2.0 mmol) in diethyl ether (25 mL) were added 2,2'-bipyridine (0.31 g, 2.0 mmol) and 1,1,1,3,3,3-hexafluoro-2-methyl-2-propanol (1.0 mL, 8.0 mmol) at room temperature. The solution turned purple immediately. After being stirred for 30 min the solution was filtered, and the filtrate was taken to dryness. The solid was extracted with toluene (50 mL), and the filtered extract was concentrated to ca. 5 mL. The precipitated solid was collected by filtration, dried under vacuum, and extracted with diethyl ether (50 mL). The filtered extract was concentrated to 30 mL and cooled to -20°C to yield purple needles. Additional crops of crystals were obtained by further concentration and cooling of the supernatant. Yield: 0.56 g (53%). IR (cm^{-1}): 1617 m, 1609 m, 1590 m, 1583 m, 1567 w, 1499 w, 1457 s, 1426 m, 1310 s, 1300 s, 1257 m, 1217 s, 1180 vs, 1110 s, 1069 s, 1047 m, 1037 m, 1023 m, 1010 w, 992 m, 961 m, 897 vw, 857 m, 810 vw, 772 s, 752 m, 706 m, 666 vw, 652 vw, 640 w, 623 w, 542 w, 531 w, 423 w. ^1H NMR (C_7D_8 , 298 K): δ 7.69 (fwhm 110 Hz, $\text{C}_{10}\text{N}_2\text{H}_8$), -3.68 (s, fwhm 830 Hz, $\text{OC}(\text{CH}_3)(\text{CF}_3)_2$).

Bis(1,1,1,3,3,3-hexafluoro-2-methyl-2-propoxo)(pyridine)copper(II) (8). **Method 1.** To a suspension of $[\text{Cu}(\text{OMe})_2]_n$ (1.0 g, 8.0 mmol) in diethyl ether (40 mL) at room temperature were added pyridine (1.28 g, 15.8 mmol) and 1,1,1,3,3,3-hexafluoro-2-methyl-2-propanol (2.0 mL, 16.0 mmol). The solution was stirred for 4 h and filtered, and the solvent was removed under vacuum. The residue was dried under vacuum overnight to yield a waxy green solid. The solid was extracted with pentane (50 mL), and the filtered extract was concentrated to ca. 15 mL and cooled to -72°C to yield a turquoise-colored powder. Yield: 0.15 g (3%). IR (cm^{-1}): 1604 m, 1483 m, 1457 s, 1295 vs, 1172 vs, 1102 vs, 1063 vs, 1041 s, 1014 m, 955 s, 851 m, 799 w, 756 s, 697 s, 632 m, 625 m, 535 m, 423 m. ^1H NMR (C_7D_8 , 293 K): δ 25.96 (s, fwhm 1550 Hz, meta CH), 12.76 (s, fwhm 240 Hz, para CH), 3.03 (s, fwhm 540 Hz, $\text{OC}(\text{CH}_3)(\text{CF}_3)_2$).

Method 2. To a suspension of CuBr_2 (0.5 g, 2.2 mmol) in tetrahydrofuran (100 mL) was added sodium 1,1,1,3,3,3-hexafluoro-2-propoxide (0.90 g, 4.4 mmol). After being stirred for 3 h, the solution turned yellow and a brown precipitate formed. The solvent was removed under vacuum, and the residue was treated with pentane (100 mL) and pyridine (0.4 mL, 4.9 mmol). After being stirred for 30 min, the resulting blue-green solution was filtered, and the filtrate was concentrated to ca. 20 mL and cooled to -20°C to yield turquoise-colored crystals. Yield: 0.56 g (44%).

Hydrolysis of 2 to Copper(II) Oxide. A solution of **2** (0.2 g, 0.4 mmol) in water (20 mL) was refluxed for 1 day, and the resulting black powder was collected by filtration and dried under vacuum. Yield: 0.04 g (ca. 100%). Anal. Calcd: C, 0; H, 0; N, 0; Cu, 79.9. Found: C, 0.84; H, 0.35; N, 0.08; Cu, 80.7.

MOCVD Studies of 2. The MOCVD apparatus has been described elsewhere.³⁹ The precursor reservoir was maintained at 70°C , the pressure

(39) Girolami, G. S.; Jensen, J. A.; Gozum, J. E.; Pollina, D. M. *Mater. Res. Soc. Symp. Proc.* **1988**, *121*, 429-438.

was 10^{-5} Torr, and the deposition zone was set at 300 °C. Approximately 0.25 g of precursor was used. The deposition time was 5 h.

Crystallographic Studies.⁴⁰ Single crystals of $\text{Cu}(\text{hfip})_2(\text{tmed})$ (**2**), grown from diethyl ether, were mounted on glass fibers with Paratone-N oil (Exxon) and immediately cooled to -75 °C in a cold nitrogen gas stream on the diffractometer. [Single crystals of $\text{Cu}(\text{hftb})_2(\text{tmed})$ (**6**), also grown from diethyl ether, were treated similarly. Subsequent comments in brackets will refer to **6**.] Standard peak search and indexing procedures gave rough cell dimensions, and the diffraction symmetry was confirmed by inspection of the axial photographs. Least-squares refinement using 25 reflections yielded the cell dimensions given in Table II.

Data were collected in one quadrant of reciprocal space ($\pm h, +k, -l$) by using the measurement parameters listed in Table II. Systematic absences for $h0l$ ($l \neq 2n$) and $0k0$ ($k \neq 2n$) were consistent only with space group $P2_1/c$. [For **6**, the systematic absences hkl ($h + k + l \neq 2n$) and $h0l$ ($l \neq 2n$) were consistent with space group $I2/a$.] The measured intensities were reduced to structure factor amplitudes and their esd's by correction for background, scan speed, and Lorentz and polarization effects. While corrections for crystal decay were unnecessary, absorption corrections were applied; the maximum and minimum transmission factors were 0.697 and 0.646 [0.881 and 0.738]. Systematically absent reflections were deleted, and symmetry-equivalent reflections were averaged to yield the set of unique data. Only those data with $I > 2.58\sigma(I)$ were used in the least-squares refinement.

The structure was solved using direct methods (SHELX-86). The correct positions for all non-hydrogen atoms (except C9 and C10) were deduced from an E map. Subsequent least-squares refinement and difference Fourier calculations revealed the positions of C9, C10, H1, and H4. All remaining hydrogen atoms were included as fixed contributors in "idealized" positions. Although molecules of **2** possess nearly ideal 2-fold symmetry, it is clear from the unambiguously determined space group and the well-behaved features of the final model that molecules of **2** do in fact lie on general positions and that no higher crystallographic symmetry is present. [For **6**, the correct non-hydrogen atoms were deduced from a vector map. Subsequent least-squares refinement and difference Fourier calculations revealed positions for all the hydrogen atoms.] The

quantity minimized by the least-squares program was $\sum w(|F_o| - |F_c|)^2$, where $w = 1.77/(\sigma(F_o)^2 + pF_o^2)$. [For **6**, $w = 1.22/(\sigma(F_o)^2 + pF_o^2)$.] The analytical approximations to the scattering factors were used, and all structure factors were corrected for both real and imaginary components of anomalous dispersion. In the final cycle of least-squares refinement, anisotropic thermal coefficients were refined for the non-hydrogen atoms, a common isotropic thermal parameter was refined for hydrogen atoms H1 and H4, and a separate common isotropic thermal parameter was refined for the remaining hydrogen atoms. No correction for extinction was necessary. [For **6**, anisotropic thermal coefficients were refined for the non-hydrogen atoms, independent isotropic thermal coefficients were refined for hydrogen atoms, and an isotropic extinction parameter was refined to a final value of 1.29×10^{-7} .] Successful convergence was indicated by the maximum shift/error of 0.002 [0.064] for the last cycle. Final refinement parameters are given in Table II. There were no significant features in the final difference Fourier map. A final analysis of variance between observed and calculated structure factors showed no apparent errors.

Acknowledgment. We thank the Department of Energy (Contract DE-AC 02-76 ER 1198) and the National Science Foundation (Grant DMR 88-09854) through the Science and Technology Center for Superconductivity for funding. XPS and XRD data were collected at the Center for Microanalysis of Materials, University of Illinois, which is supported by the U.S. Department of Energy under Contract DE-AC 02-76ER 01198. SEM studies were performed at the Center for Electron Microscopy, University of Illinois. We particularly thank Ms. Teresa Prussak-Wieckowska of the University of Illinois X-ray Crystallographic Laboratory for assistance with the crystallographic studies. P.M.J. is the recipient of a University of Illinois Department of Chemistry Fellowship. G.S.G. is the recipient of an A. P. Sloan Foundation Research Fellowship and a Henry and Camille Dreyfus Teacher-Scholar Award.

Supplementary Material Available: Tables of final atomic coordinates, anisotropic thermal parameters, and complete bond distances and angles for **2** and **6** and a table of calculated hydrogen atom positions for **2** (9 pages). Ordering information is given on any current masthead page.

(40) For details of the data collection and refining procedures see: Jensen, J. A.; Wilson, S. R.; Girolami, G. S. *J. Am. Chem. Soc.* **1988**, *110*, 4977-4982.